

## Digital isochrons of the world's ocean floor

R. Dietmar Müller,<sup>1</sup> Walter R. Roest,<sup>2</sup> Jean-Yves Royer,<sup>1,3</sup> Lisa M. Gahagan,<sup>4</sup> and John G. Sclater<sup>5</sup>

**Abstract.** We have created a digital age grid of the ocean floor with a grid node interval of 6 arc min using a self-consistent set of global isochrons and associated plate reconstruction poles. The age at each grid node was determined by linear interpolation between adjacent isochrons in the direction of spreading. Ages for ocean floor between the oldest identified magnetic anomalies and continental crust were interpolated by estimating the ages of passive continental margin segments from geological data and published plate models. We have constructed an age grid with error estimates for each grid cell as a function of (1) the error of ocean floor ages identified from magnetic anomalies along ship tracks and the age of the corresponding grid cells in our age grid, (2) the distance of a given grid cell to the nearest magnetic anomaly identification, and (3) the gradient of the age grid: i.e., larger errors are associated with high age gradients at fracture zones or other age discontinuities. Future applications of this digital grid include studies of the thermal and elastic structure of the lithosphere, the heat loss of the Earth, ridge-push forces through time, asymmetry of spreading, and providing constraints for seismic tomography and mantle convection models.

### Introduction

The age of the ocean floor is an important parameter in the study of plate tectonic processes. An accurate digital age grid is essential for many studies, including plate kinematics, studies of plate driving forces, mantle dynamics, ocean floor roughness, and paleoceanography. Several analog maps of the age of the ocean floor have been compiled using magnetic anomaly data [e.g., Sclater *et al.*, 1981; Larson *et al.*, 1985]. A digital version of the latter map was produced by Cazenave *et al.* [1988], at a grid interval of 0.5 degrees (approximately 55 km). Recent improvements in identifications of magnetic anomalies and plate kinematic models, especially aided by dense gravity data from satellite altimetry, permit a more detailed description of the spreading process and have initiated the construction of a more detailed age grid.

### Ocean Floor Isochrons and Plate Boundaries

We have constructed a global set of isochrons for the ocean basins corresponding to magnetic anomalies 5, 6, 13, 18, 21, 25, 31, 34, M0, M4, M10, M16, M21, and M25 based on a global plate reconstruction model, magnetic anomaly identifications and fracture zones [see also Royer *et al.*, 1992]. The geomagnetic timescale of Cande and Kent [1995] was used for anomalies younger than chron 34 (83 Ma), the timescale from Gradstein *et al.* [1994] for older times. Isochrons were constructed by plotting reconstructed magnetic anomaly and fracture zone picks, as well as selected small circles computed

from stage rotation poles for each isochron time, keeping one plate fixed. Then best fit continuous isochrons were constructed, connected by transforms, in the framework of one fixed plate [see also Müller *et al.*, 1991]. A complete set of isochrons for all conjugate plate pairs was derived by rotation of every isochron to their present-day position.

Construction of a complete age grid also requires knowledge of the present day plate boundary geometry. The boundaries shown in Plate 1 have been compiled based on a marine gravity grid from Geosat exact repeat mission, Geodetic Mission, and ERS-1 satellite altimetry data [Sandwell *et al.*, 1994], bathymetric data, and earthquake epicenters. There is a substantial area of ocean floor that is older than the oldest mapped isochrons. In order to estimate ages for the oldest ocean floor in ocean basins bounded by passive margins, we assigned ages to continental margin segments based on geological data and published plate models. The regional boundaries between continental and oceanic crust have been compiled by Müller and Roest [1992] (North and central North Atlantic), Nürnberg and Müller [1991] (South Atlantic), and Royer *et al.* [1992] (Indian Ocean). South of 60°S a dense grid of Geosat Geodetic Mission data [Sandwell *et al.*, 1994] has been used to better locate boundaries between continental and oceanic crust of the Antarctic continental margin.

### Interpolation of Isochrons and Gridding

In order to create a smooth grid of ocean floor ages that maintains all sharp age discontinuities at fracture zones, we first create a set of densely interpolated isochrons. We assume that the spreading direction between two adjacent isochrons is given by a constant stage pole of motion, derived from our plate kinematic model. We also assume that the spreading velocity between two adjacent isochrons is constant, and that consequently the age varies linearly in the direction of spreading on a given ridge flank. To simplify the calculations, each pair of adjacent isochrons is transformed to a coordinate system in which the stage pole of motion between the two isochrons is moved onto the geographic north pole [Roest *et al.*, 1992]. Then intermediate isochrons were

<sup>1</sup> Department of Geology and Geophysics, University of Sydney, New South Wales, Australia.

<sup>2</sup> Geological Survey of Canada, Ottawa.

<sup>3</sup> Géosciences Azur, Villefranche Sur Mer, France.

<sup>4</sup> Institute for Geophysics, University of Texas at Austin.

<sup>5</sup> Scripps Institution of Oceanography, University of California, San Diego.

Copyright 1997 by the American Geophysical Union.

Paper number 96JB01781.  
0148-0227/97/96JB-01781\$09.00

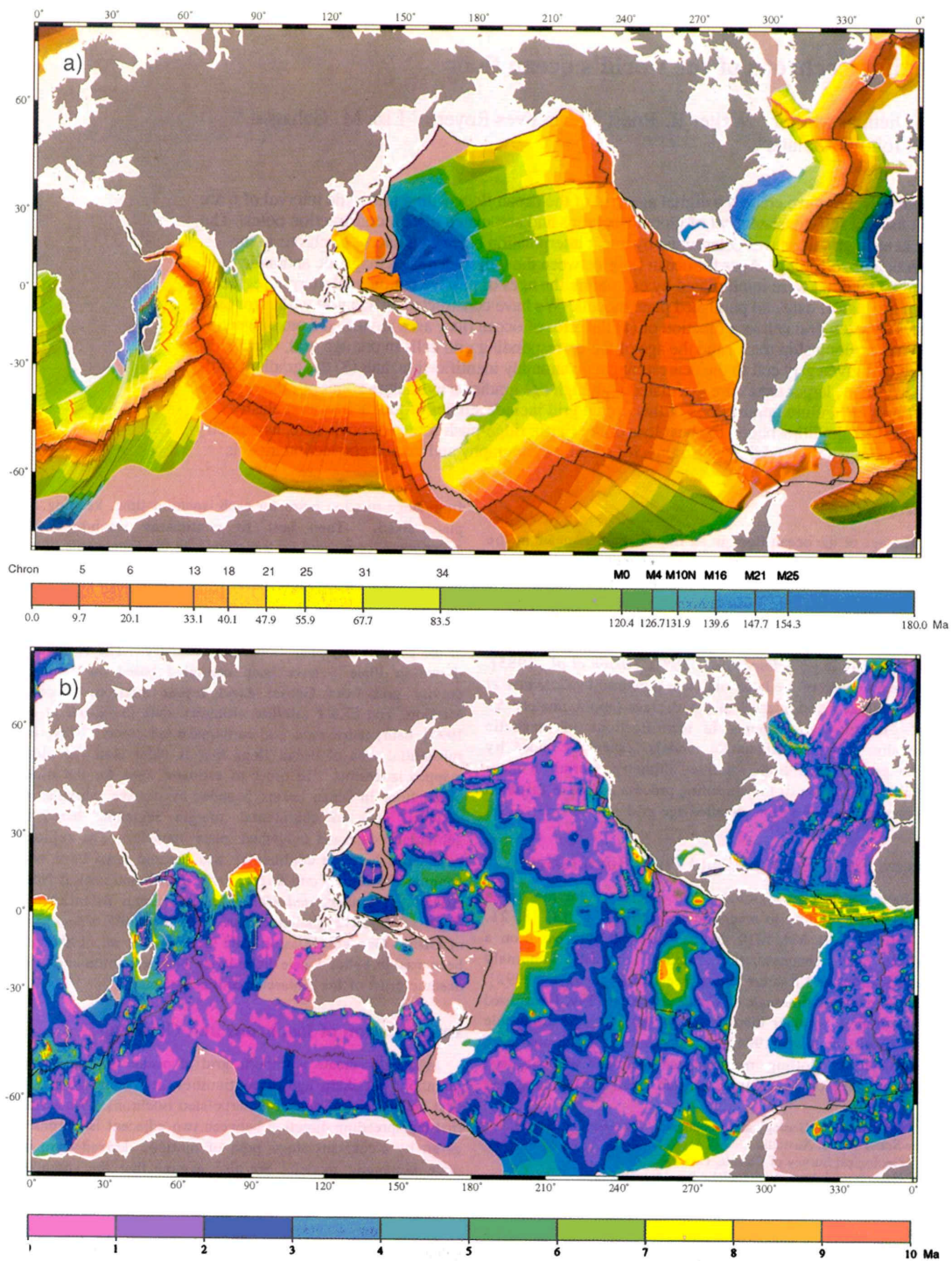


**Plate 1.** (a) Color shaded relief map, illuminated from the northwest, displaying the ages of the ocean floor. (b) Gridded estimates for age uncertainties including (1) the error of ocean floor ages identified from magnetic anomalies along ship tracks and the age of the corresponding grid cells in our age grid, (2) the distance of a given grid cell to the nearest magnetic anomaly identification, and (3) large gradients of the age grid near fracture zones.

linearly interpolated along plate flow lines. This is equivalent to interpolation along small circles about the stage pole. The complete set of isochrons for each stage was subsequently rotated back into the geographic reference frame. This was done for each isochron pair on each plate pair.

To interpolate the ages onto a regular grid, we assume that the isochrons are continuous, which is implemented by densely interpolating between observation points along each isochron. A minimum curvature routine is used to obtain age values on a regular grid at a resolution of 0.1 degrees, equivalent to 6 arc min. Areas of the ocean floor with insufficient data coverage were blanked out in the grid. We included data from selected back-arc basins, where data coverage is sufficient and available to us. The resolution of our grid for these areas is typically reduced by a factor of 10 with respect to the oceanic grid, i.e., the resolution in back-arc basins does not exceed 1 degree, and provides merely a rough estimate of the age distribution in these basins. The resulting grid is shown in Plate 1a.

### Accuracy

The accuracy of the age grid varies considerably because of the spatially irregular distribution of ship track data in the oceans. Other sources of errors are given by our chosen spacing of isochrons as listed before, between which we interpolated linearly. These stages are especially long during long time intervals without changes in the polarity of the Earth's magnetic field such as the Cretaceous Magnetic Quiet Zone from about 118 to 83 Ma. We assume that age grid errors depend on the distance to the nearest data points and the proximity to fracture zones. In order to estimate the accuracy of our age grid, we construct a grid with age-error estimates for each grid cell dependent on (1) the error of ocean floor ages identified from magnetic anomalies along ship tracks and the age of the corresponding grid cells in our age grid, (2) the distance of a given grid node to the nearest magnetic anomaly identification, and (3) the gradient of the age grid: i.e., larger errors are associated with high age gradients across fracture zones or other age discontinuities. The latter also reflects that, because of the interpolation process, uncertainty in the magnetic anomaly will induce larger age errors in regions of slow spreading rates than in regions of fast spreading rates.

We first compute the age differences between ~30,000 interpreted magnetic anomaly ages and the ages from our digital age grid, and investigate the size and distribution of the resulting age errors. We find that the majority of errors are smaller than 1 m.y. and errors larger than 10 m.y. are mostly due to erroneously labeled or interpreted data points. Therefore we set an upper limit for acceptable errors as 10 m.y. As a lower limit we arbitrarily choose 0.5 m.y., since we do not expect to resolve errors smaller than 0.5 m.y. given the uncertainty in the timescales used. We grid the remaining age errors by using continuous curvature splines in tension.

The constraints on the ages in our global age grid generally decrease with increasing distance to the nearest interpreted magnetic anomaly data point. Areas without interpreted magnetic anomalies include east-west spreading mid-ocean ridges in low latitudes such as the equatorial Atlantic ocean, where the remanent magnetic field vectors are nearly parallel to the mid-ocean ridge and cause very small magnetic anomalies, and areas with sparse data coverage such as some remote areas in the southern ocean. In order to address the "tectonic reconstruction uncertainties" for these areas, we

create a grid containing the distance of a given grid cell to the nearest data point, ranging from zero at the magnetic anomaly data points to 10 at distances of 1000 km and larger. We smooth this grid using a cosine arch filter (5 degrees full width) and add the result to the initial splined grid of age errors.

Fracture zones are usually several tens of km wide, containing highly fractured and/or serpentinized ocean crust. Age estimates may be uncertain especially near large-offset fracture zones, which are more severely affected by changes in spreading direction than small-offset fracture zones. Consequently, our age estimates along large-offset fracture zones may be more uncertain than at small-offset fracture zones or on "normal" ocean crust. Large-offset fracture zones are easily identified in the age grid by computing the gradient of the age grid. We identify the age gradients associated with medium- to large-offset fracture zones, set the gradients of "normal" ocean crust to zero, smooth the result with a 3x3 moving average filter, and scale the grid to range from one to two. After multiplying the error grid with the smoothed age gradients along fracture zones, we have not altered the errors associated with "normal" ocean floor, and increased the errors at fracture zones by a factor between 1 and 2, depending on the magnitude of the age gradient. The resulting grid of age uncertainties is shown in Plate 1b.

### Conclusions

The digital age grid presented here is the first of its kind, because (1) in the past ages of the ocean floor have only been available on analog maps, with the exception of a digitized version of *Larson et al.*'s [1985] age map produced by *Cazenave et al.* [1988] at a relatively coarse grid interval of 0.5 degrees, (2) our grid is based on a self-consistent global plate model, and (3) it is accompanied by a grid estimating the uncertainties of the gridded ages. A shortcoming of our error analysis at present is that it does not include the uncertainties of the plate rotations. We hope to include this parameter in the next age grid generation.

### Appendix

The digital age and age-error grids as well as background information on details of the data sources and plate model the age grid is based on can be obtained through the World Wide Web site of the University of Sydney Department of Geology and Geophysics at <http://www.es.su.oz.au/agegrid/agegrid.html>. Information on how to obtain posters of the age grid can be found at <http://gdinfo.agg.nrcan.gc.ca/app/agegrid.html> and [http://www.ngdc.noaa.gov/mgg/announcements/announce\\_crustage.html](http://www.ngdc.noaa.gov/mgg/announcements/announce_crustage.html)

**Acknowledgments.** This work was made possible by the contributors to the former Paleooceanographic Mapping Project (POMP, University of Texas, Austin) who released data that served as partial input for constructing the isochrons, POMP industry sponsors for financial support to R.D.M., L.M.G. and J-Y.R., and by the PLATES industry sponsors through support to L.M.G. Construction of the age grid was started at the Scripps Institute of Oceanography while the senior author was supported by a graduate and a postdoctoral fellowship. JYR acknowledges support by the CNRS (Centre National de la Recherche Scientifique). The GMT software system from P. Wessel and W.H.F. Smith was invaluable in performing the age error analysis, and for producing the figures. Careful reviews by Anne Cazenave, Roger Larson, and James Ogg helped clarify the manuscript. UMR Géosciences Azur contribution 54, Geological Survey of Canada contribution 1996353.

## References

- Cande, S.C., and D.V. Kent, Revised calibration of the geomagnetic time scale for the late Cretaceous and Cenozoic, *J. Geophys. Res.*, **100**, 6093-6098, 1995.
- Cazenave, A., K. Domih, M. Rabinowicz, and G. Ceuleneer, Geoid and depth anomalies over ocean swells and troughs: evidence of an increasing trend of the geoid to depth ratio with age of plate, *J. Geophys. Res.*, **93**, 8064-8077, 1988.
- Gradstein, F.M., F.P. Agterberg, J.G. Ogg, J. Hardenbol, P. van Veen, J. Thierry, and Z. Huang, A Mesozoic timescale, *J. Geophys. Res.*, **99**, 24,051-24,074, 1994.
- Larson, R.L., W.C. Pitman, X. Golovchenko, S.D. Cande, J.F. Dewey, W.F. Haxby, and J.L. LaBrecque, *Bedrock Geology of the World*, W.H. Freeman, New York, 1985.
- Müller, R.D. and W.R. Roest, Fracture zones in the North Atlantic from combined Geosat and Seasat data, *J. Geophys. Res.*, **97**, 3337-3350, 1992.
- Müller, R. D., D.T. Sandwell, B.E. Tucholke, J. G. Sclater, and P.R. Shaw, Depth to basement and geoid expression of the Kane Fracture Zone: a comparison, *Mar. Geophys. Res.*, **13**, 105-129, 1991.
- Nürnberg, D. and R.D. Müller, The tectonic evolution of the South Atlantic from Late Jurassic to Present, *Tectonophysics*, **191**, 27-53, 1991.
- Roest, W.R., R.D. Müller, and J. Verhoef, Age of the ocean floor: A digital data set for the Labrador Sea and Western North Atlantic, *Geosci. Can.*, **19**, 27-32, 1992.
- Royer, J.-Y., R.D. Müller, L.M. Gahagan, L.A., Lawver, C.L. Mayes, D. Nürnberg, and J.G. Sclater, A global isochron chart, *Tech. Rep. 117*, Austin, Univ. of Tex. Inst. for Geophys., 1992.
- Sandwell, D.T., M. Yale, and W.H.F. Smith, ERS-1 geodetic mission reveals detailed tectonic structures, *EOS Trans. AGU*, **75 (44)**, Fall Meet. Suppl., 155, 1994.
- Sclater, J.G., B. Parsons, and C. Jaupart, Oceans and continents: Similarities and differences in the mechanism of heat loss, *J. Geophys. Res.*, **86**, 11,535 - 11,552, 1981.
- L. M. Gahagan, Institute for Geophysics, University of Texas at Austin, 8701 Mopac Boulevard, Austin, TX 78759-8345. (e-mail: lisa@utig.ig.utexas.edu)
- R. D. Müller, Department of Geology and Geophysics, Building F05, University of Sydney, New South Wales, 2006, Australia. (e-mail: dietmar@es.su.oz.au)
- W. R. Roest, Geological Survey of Canada, 1 Observatory Crescent, Ottawa, Canada K1A 0Y3. (e-mail: roest@agg.emr.ca)
- J.-Y. Royer, Géosciences Azur, La Darse - B.P. 48, 06235 Villefranche Sur Mer cedex, France (e-mail: royer@ccrv.obs-vlfr.fr)
- J. G. Sclater, Scripps Institution of Oceanography, UCSD, 9500 Gilman Drive, La Jolla, CA 92093-0215. (e-mail: sclater@bullard.ucsd.edu)

(Received July 24, 1995; revised April 12, 1996;  
accepted June 4, 1996.)